Available online at www.sciencedirect.com
ScienceDirect
Journal of Photochemistry and Photobiology A: Chemistry 197 (2008) 321–328
Journal of Photochemistry and Photobiology A:Chemistry
www.elsevier.com/locate/jphotochem

The photocatalytic activity of TiO_2 foam and surface modified binary oxide titania nanoparticles

A.O. Ibhadon [a,*], G.M. Greenway [b], Y. Yue [b], P. Falaras [c], D. Tsoukleris [c]

[a] *Faculty of Science and Environment and Hull Environment Research Institute, University of Hull, Cottingham Road, Hull HU6 7RX, United Kingdom*
[b] *Department of Chemistry, Faculty of Science and Environment, University of Hull, Cottingham Road, Hull HU6 7RX, United Kingdom*
[c] *National Centre for Scientific Research, Institute of Physical Chemistry, Athens, Greece*

Received 7 December 2007; received in revised form 23 January 2008; accepted 28 January 2008
Available online 6 February 2008

Abstract

Surface modified titania dioxide composite nanoparticles prepared by hydrogen reduction reaction and a mesoporous TiO_2 foam made from a surface modifier and a long chain organic surfactant were characterized by diffractive, spectroscopic and microscopic techniques and studied for their catalytic activity towards the decomposition of an industrial water pollutant, methyl orange. The surface deposition of ruthenium and silicon particles improved the photocatalytic activity of the composite particles resulting in a faster decomposition of the methyl orange compared to commercial TiO_2 alone. Modification of TiO_2 with RuO_2 only offered a marginal benefit over TiO_2 while the incorporation of RuO_2 and SiO_2 into TiO_2 resulted in a marked increase in the rate constant and catalytic activity. These results are consistent with the enhanced surface properties of the composite materials resulting from the modification of TiO_2 with RuO_2 and SiO_2. This surface enhancement effects appear synergetic to the charge separation process and hence the photocatalytic results are explained on the basis of a mechanism involving efficient charge transfer across the interfaces of the composites involving photogenerated electron–hole pairs. Results obtained in this study show that the percentage degradation after 1 h of illumination was 47.15% for TiO_2 foam, 75.5 and 106.4%, respectively, for TiO_2/RuO_2 (SiO_2 5%, w/w) and TiO_2/RuO_2(SiO_2 10%, w/w) and 34.15% for commercial TiO_2.

Keywords: Foam; Spectroscopy; Composites; Nanoparticles; X-ray diffraction; SEM microscopy

1. Introduction

Due to its ability to degrade a variety of toxic organic compounds in air and water, TiO_2 remains the most frequently studied semiconductor photocatalyst. Many reviews of different aspects of single-crystalline metal oxide surfaces have been reported [1–4] and significant research efforts using a variety of analytical methods have been devoted to study various TiO_2 surfaces [5–8]. TiO_2 surfaces for films and particles have become model systems in the science of metal oxide surfaces because reduced TiO_2 single crystals are easy to work with and the growth morphology, interfacial oxidation and reduction reaction, thermal stability and geometric structure of surface are the critical parameters on which the reactivity of these materials depends [8].

Modifications of semiconductor surfaces by the addition of metal ions, binary or tertiary metal oxides is beneficial in decreasing the electron–hole recombination rate and thereby increasing the efficiency of the catalyst towards the degradation of a host of water and air pollutants [8]. Metal-doping of semiconductors decreases the band gap energy and increases the photocatalytic activity of titania by enhancing its surface properties and generating a 'barrier' which acts as an electron trap for the metal in contact with the semiconductor surface. Similarly, modification of semiconductors with transition metal ions improves the trapping of electron and inhibits electron–hole recombination because the low photoactivity of titania is due to the fast recombination of photogenerated electrons and holes.

* Corresponding author. Tel.: +44 1723 357318.
E-mail address: a.o.ibhadon@hull.ac.uk (A.O. Ibhadon).

1010-6030/$ – see front matter © 2008 Elsevier B.V. All rights reserved.
doi:10.1016/j.jphotochem.2008.01.010

In recent years, researchers have focused on the combination of different kinds of metallic oxide particles including the ruthenium–titanium metallic oxides, known for many years to be very active catalysts. The presence of SiO_2 in TiO_2/RuO_2 leads to an increase in the effective surface area of titania and helps to promote the efficiency of the photocatalyst [9–12].

Methyl orange (MO) is an intensely colored compound used in dyeing, foodstuff, paper and pulp, leather and printing textiles and is thus a common water pollutant in these industries. The release of these materials and their products into the environment creates major problems and so there are intense research efforts aimed at the decolorization of these dyes [13–15]. The aim of this study was to modify the surface properties of pure TiO_2 by incorporating RuO_2 and SiO_2 into it and evaluate the catalytic activity of the resulting materials towards the decomposition of this pollutant. The study also investigates the degradation of methyl orange using a porous TiO_2 foam prepared from a long chain surfactant and a surface modifier and compares with the activity of the nanoparticles. This would enable the identification of key parameters such as coating thickness, particle size, surface area, pore size and crystal phase, that can be experimentally manipulated to control photoactivity as studies have shown that photoactivity is dependent on processing conditions and the surface morphology of catalyst materials.

2. Experimental

The pollutant used in this work was methyl orange, which has the formula (4-[[(4-dime thyamino)phenyl]-azo]benzenesulfonic acid sodium salt) and molecular formula $[(CH_3)_2NC_6H_4N{=}NC_6H_4SO_3Na]$ or Acid Orange 52, obtained from Merck and was used without further purification. It is a stable compound and a typical azo-dye in the textile industry and the subject of previous studies [16,17]. Analytical grade hydrogen peroxide and acetylacetone were obtained from Fisher Scientific Ltd., UK. Hexadecylamine (HDA) was obtained from Fluka while Degussa P-25 was kindly supplied by Degussa AG, Macclesfield, England, United Kingdom.

2.1. Preparation of TiO_2 foam

A detailed procedure for preparing the TiO_2 foam is provided in [18]. Two grams of 1-hexadecylamine (HDA) (Fluka, Assay, >99%), was dissolved in 4 ml aqueous solution of boiling acetone. The elevated solvent temperature ensured the necessary solubility of the organic surfactant. While the solution was still hot, 1 g of TiO_2 (Degussa P-25) and 50 ml of 30% H_2O_2, were added. The long-chain amine (HDA), apart from the ampiphilic character of the molecule, provided the necessary alkalinity for the hydrogen peroxide to decompose to O_2 bubbles. Following the H_2O_2 addition, the volume increased rapidly to 150 ml after 1 h, resulting in the formation of a yellow, and highly porous TiO_2 foam material. The titania foam was dried at ambient temperature for 2 days, before storing under vacuum at 20 mbar in a powder form. 'Foam' as used in this study actually refers to the process of formation of the final titania material rather than the actual material itself. The 'foam' is not a structured support or a reticulated foam. It can actually be crushed into powder or fine particles.

2.2. Characterization of the foam

The structure of the titania foam resembles a network of interconnected flakes forming irregular polygonal cavities of 500 nm in size. Detailed surface images of the foam were obtained by means of a scanning electron microscope (SEM) with numerical image acquisition (LEICA S440). Carbon deposition was performed to avoid problems arising from surface charge effects. X-ray from the SEM microscope probe at horizontal incidence beam was used for non-destructive qualitative and quantitative chemical analysis of the foam.

The crystallinity of the foam was studied with a Siemens D-500 X-ray diffractometer (XRD, Siemens D-500, Cu Kα radiation) using Cu Kα radiation. To discriminate the local order characteristics of the TIO_2 foam, a non-resonant Raman Spectroscopy, employing a triple Jobin–Yvon spectrometer (DILOR OMARS 89 spectrometer) equipped with a microscope, a CCD detector and a 514.5 nm argon laser, was used, Fig. 3.

2.3. Preparation of $TiO_2/SiO_2/RuO_2$ nanoparticles

$TiO_2/RuO_2/SiO_2$ nanoparticles were prepared by mixing 10 g TiO_2 and 1 g SiO_2 powders with 10 ml of water to form a composite of TiO_2/SiO_2 (90%:10%, w/w). Based on the TiO_2 (90%)–(10%, w/w) SiO_2 composite, a controlled impregnation technique was used to prepare composite particles of TiO_2/RuO_2 (with SiO_2 content from 5 to 10%, w/w) of various thicknesses. The TiO_2–SiO_2 (10%, w/w) powder mixture was placed in a 1 mg/l $RuCl_3$ solution. After the $RuCl_3$ solution has been absorbed completely into the SiO_2–TiO_2 mixture, the $RuCl_3/TiO_2$-SiO_2 catalysts were annealed in an oven at 600 °C for 15 h [19].

2.4. Surface area and porosity measurement

Surface area measurements of the nanoparticles was carried out using Micromeritics Analyzer, Tri-Star 3000, which used physical adsorption and capillary condensation principles to obtain information the surface area and porosity of the nanoparticles. The surface properties of Degussa P-25, TiO_2/RuO_2, and TiO_2/RuO_2 with SiO_2 content from 5 to 10% (w/w) were measured.

2.5. Photocatalytic studies

To evaluate the catalytic activity of the TiO_2 foam, TiO_2 and $TiO_2/RuO_2/SiO_2$ particles towards azo-dye degradation, photocatalysis experiments were conducted in round-bottomed photocatalytic pyrex glass cells, cut off wavelength 320 nm and MO was the model pollutant used. Previous studies have indicated that this azo-dye was not decomposed even after prolonged periods of irradiation in the absence of a photocatalyst [20]. It was therefore considered appropriate to express the photocatalytic activity as a percentage of the disappearance of this

pollutant measured as changes in the characteristic peak intensity with time.

To 250 ml of dye solution containing 5 mg/l methyl orange, the modified titania photocatalyst (0.2 g foam) was added and the suspension was subjected to irradiation. The irradiation system is equipped with two parallel F15 W/T8 UV light tubes which have maximum emission at 350 nm. The radiation from the system was measured using a 28-0925 Ealing Research Radiometer–Photometer operating in conjunction with a 28-0982 silicon detector and a 28-0727 flat response filter. Aqueous solutions of methyl orange were photocatalysed using different loads (initial load of 10% SiO_2, 90% TiO_2) of the composite nanoparticles of RuO_2 and $TiO_2/RuO_2/SiO_2$ and the TiO_2 foam (0.2 g), particle size 500 nm [18]. All solutions were O_2 bubbled to achieve dissolved oxygen saturation and spectrophotometrical analytical determination was carried out at 465 nm (MO = 25,100 M^{-1} cm^{-1}) and constant stirring was achieved using magnetic stirrers. At different time intervals, an aliquot from the solution was syringed from the solution and filtered through Millipore Syringe filter of 0.45 μm. The absorption spectra was then recorded and the rate of decolorization was determined from the change in intensity of λ_{max} of the MO. Initial pollutant concentration and pH were set at 5 mg/l and pH 8 as previous studies on MO indicated that the progress of decomposition can be followed easily at this concentration and pH [20]. The photocatalytic decomposition rate was determined from the following equation [21].

$$\text{Photocatalytic decomposition rate} = \frac{C_0 - C}{C_0} \quad (1a)$$

where C_0 is the initial concentration of the methyl orange solution and C is the final concentration after illumination by UV light. This enabled us to determine the decolorization efficiency (%) according to the equation:

$$\text{Efficiency } (\%) = \frac{C_0 - C}{C_0} \times 100 \quad (1b)$$

3. Results and discussions

3.1. Characterization of TiO_2 nanoparticles

Table 1 shows the surface area properties of the nanoparticles. The data shows that TiO_2 (Degussa P-25) has the largest surface area and the smallest pore size. Modification of semiconductors by incorporating binary metal oxides has been shown to increase the surface area of TiO_2 [22].

Table 1
Surface properties of $RuO_2/SiO_2/TiO_2$ and Degussa P-25 TiO_2

Sample	Surface area (m^2/g)	Pore volume (cm^3/g)	Pore size (nm)
TiO_2 (Degussa) (100%)	17.49	0.055	5.60
RuO_2/TiO_2 (5% RuO_2)	18.10	0.062	6.70
$RuO_2/SiO_2/TiO_2$ (5% SiO_2)	19.22	0.059	6.75
SiO_2/TiO_2 (10% SiO_2)	21.65	0.055	7.35
$RuO_2/SiO_2/TiO_2$ (10% SiO_2)	22.08	0.052	7.53

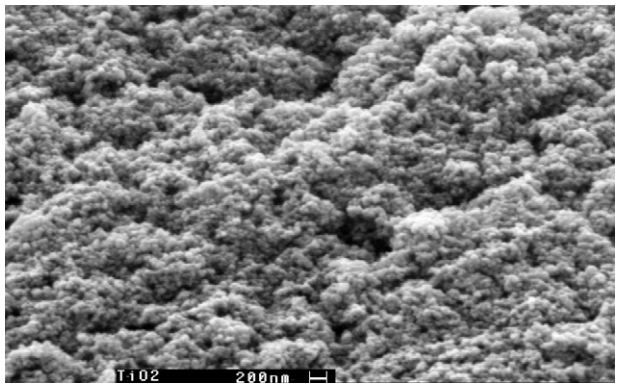

Fig. 1. SEM image of the TiO_2–HDA foam.

3.2. Characterization of titania foam

Fig. 1 shows a scanning electron microscopy image of the titania foam, revealing a spongy, rough and porous microstructure. Low magnification image of the foam presents an extended network of features separated by large pores with a diameter of 1–2 μm approximately. By increasing the SEM magnification, the fine texture of the foam features can be seen. No existence of grainy matter was observed, demonstrating that a complete reaction had occurred. The structure resembles a network of particles of 500 nm in size, where walls with thickness of about 100 nm are visible. The XRD diffractive analysis in Fig. 2 shows the anatase (A) and rutile (R) peaks at 1 0 1 and 1 1 0 reflections. The photocatalytic activity of titania is due to the anatase phase [23] which judging from the XRD results, was fully formed in the TiO_2 foam as the peaks are clearly distinguishable.

3.3. Raman spectroscopy

Raman spectroscopy is a non-destructive technique and is capable of elucidating the structural complexity of semiconductor surfaces and other materials as peaks from each crystalline phase can be separated in frequency making the anatase and

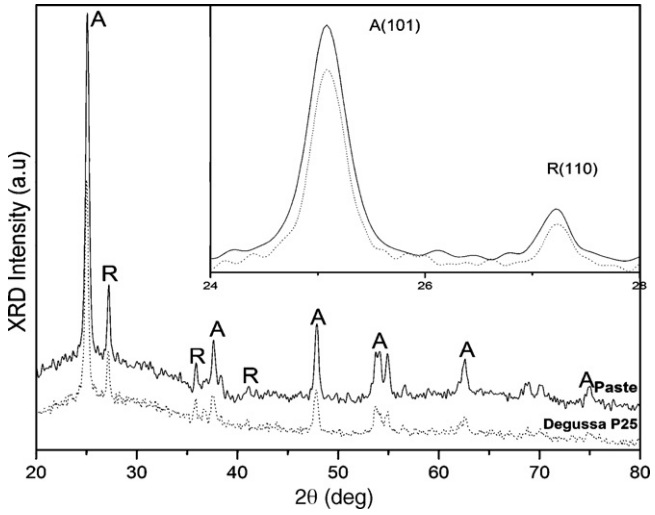

Fig. 2. XRD of TiO_2 foam.

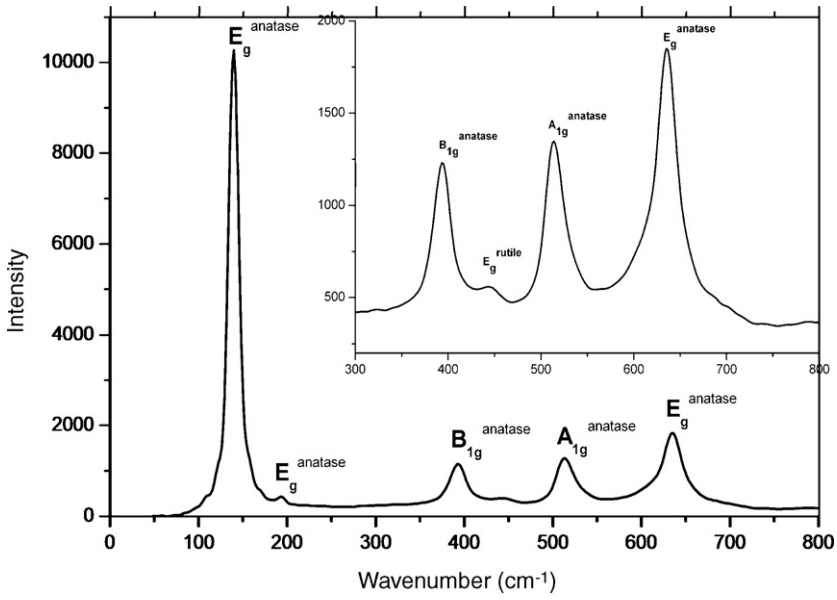

Fig. 3. Raman spectrum of TiO_2 foam.

rutile phases easily distinguishable [24]. The Raman spectra, Fig. 3, show that the foam is well crystallized as the rutile and anatase phases are clearly obvious as shown also in the X-ray diffraction data. There are no overlapping broad peaks and the vibration peaks at 393, 514, 637 cm^{-1} and 414, 525, 660 cm^{-1} due to the Degussa P-25 and the TiO_2 foam, respectively, are unambiguously attributed to the anatase modification. Although the anatase phase is the predominant specie, the rutile phase is observed as a broad peak at 446 cm^{-1} for the Degussa P-25 sample. The presence of this peak is attributed to the initial composition of the TiO_2 powder (rutile/anatase). In the TiO_2 foam, these peaks are more intense and slightly shifted to higher frequencies, due to smaller size particles [25,26].

3.4. Differential scanning calorimetry

To characterize the position of the hexadecylamine in the foam structure, a differential scanning calorimeter (DSC, TA Instruments 2920, heating rate, 2 °C/min) was used (full details given elsewhere [18]). The DSC profiles reveal that the TiO_2 foam is stable until 190 °C where an irreversible destruction takes place. DSC analysis suggests that the HDA forming the backbone of the lamellar structure of the foam is un-affected by the photocatalytic experiment carried out at room temperature in aqueous solution, the reversible melting enthalpies being 12.99 and 11.04 J/g at 57 and 54 °C, respectively [18].

3.5. Photocatalytic studies

Photocatalytic experiments were undertaken to evaluate the various TiO_2 photocatalysts as materials for water pollutant purification. The rate of decolorization was determined as a function of the change in intensity of the absorption peak at 463 nm with time. The absorption peak of the dye diminished with time and finally disappeared during the course of the reaction which indicated that the dye had been degraded. The photocatalytic decolorization of the dye is initiated by photoexcitation of the semiconductor and the formation of electron hole pairs on the surface of the catalyst, Eq. (2). The high oxidative potential of the hole (h^+_{VB}) in the catalyst allows the direct oxidation of the dye to reactive intermediates, Eq. (3)

$$\frac{MO}{MO_2} + h\nu \rightarrow \left(\frac{MO}{MO_2}\right)(e^-_{CB} + h^+_{VB}) \quad (2)$$

$$h{+}_{VB} + \text{dye} \rightarrow \text{dye}^{\cdot +} \rightarrow \text{oxidation of dye} \quad (3)$$

Another reactive intermediate responsible for the degradation of MO is the hydroxyl radical ($OH^\bullet$) formed either by the decomposition of water, Eq. (3) or by the reaction of a hole with OH^-, Eq. (4). The hydroxyl radical is a powerful non-selective oxidant with ($E_0 = +3.06$ V) the use of which can lead to the partial or complete mineralization of a host of organic compounds [27]

$$h^+_{VB} + H_2O \rightarrow H^+ + {}^\bullet OH \quad (4)$$

$$h^+_{VB} + OH^- \rightarrow {}^\bullet H \quad (5)$$

$${}^\bullet OH + \text{dye} \rightarrow \text{degradation of dye} \quad (6)$$

We observed from previous studies of MO degradation using gold modified titanium thin films that the degradation of this pollutant fitted first order kinetics [20,28,29] and it is well established that photocatalysis experiments follow the Langmuir–Hinshelwood model, where the reaction rate, R, is proportional to the surface coverage, θ, according to the equation,

$$R = -\frac{dc}{dt} = k_r\theta = \frac{k_r KC}{1 + KC}, \quad (7)$$

where k_r is the reaction rate constant, K is the adsorption coefficient of the reactant and C is the reactant concentration. When C is very small, KC is negligible with respect to unity and Eq. (7) describes a first order kinetics. The integration of Eq. (7)

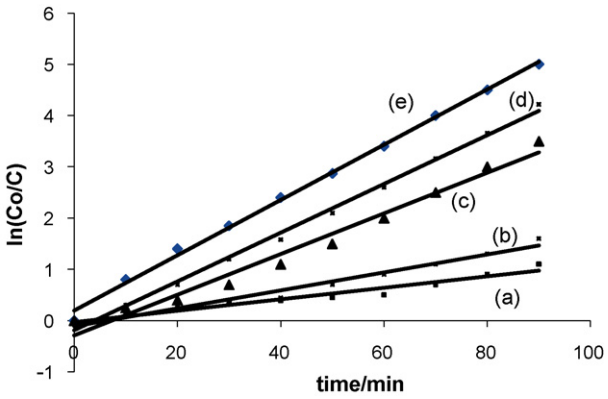

Fig. 4. Photodecomposition kinetics of 5 mg/l MO, pH 9 in (a) TiO_2/RuO_2, (b) TiO_2, (c) TiO_2/RuO_2 (5% SiO_2), (d) TiO_2/RuO_2 (10% SiO_2) and (e) TiO_2/(10% SiO_2).

with the limit conditions that at the start of radiation, $t = 0$, the concentration is the initial one, $C = C_0$, yields Eq. (8)

$$-\ln\left(\frac{C}{C_0}\right) = k_{app}t \tag{8}$$

where k_{app} is the apparent first order rate constant. Fig. 4 presents the MO degradation kinetic parameters and permits a direct comparison of the photocatalytic activities of the TiO_2 particles. Under the experimental conditions, the photocatalytic curves follow first order reaction kinetics with R^2 values approaching unity in most cases. Kinetic parameters resulting from the application of Eq. (8) are summarized in Table 2 for TiO_2 composite catalysts, TiO_2 foam and pure TiO_2. The data presented in Fig. 1 and Table 2 show that the modified materials are more effective photocatalysts compared to pure TiO_2.

We have carried out the degradation of many water and air pollutants using various modified TiO_2 catalysts [20,28–29] and have come to similar conclusions. Photocatalysis is a surface process and the kinetic parameters obtained depend on the actual surface of the semiconductor exposed to radiation. For example, immobilized TiO_2 films possess the same porous surface, however only a part of the photocatalyst surface is available for the catalytic reaction. In addition, light interactions are not negligible and in the case of nanoparticles, the packing of the particles in $TiO_2/RuO_2/SiO_2$ does not permit all photons, because of scattering effect, to reach every part of the catalyst surface.

These results though interesting, should be interpreted with some caution. This is because the data are valid for the initial rate of degradation. It has been reported that as the reaction progresses, the KC term in Eq. (7) is no longer negligible and the Langmuir–Hinshelwood kinetic model is not sufficient under this scenario to explain the observed kinetics [30].

A more appropriate approach to the analysis of photocatalytic data might be to develop a novel kinetic parameter to explain the degradation efficiency per unit area of the catalyst [30]. This factor, k_{surf}, can be derived by dividing the apparent rate constant with the surface area of the catalyst as in Eq. (9).

$$K_{surf} = \frac{K_{app}}{S} \tag{9}$$

where K_{surf} ($min^{-1}\,cm^{-2}$), is the novel parameter, k_{app} (min^{-1}), is the rate constant and S (cm^2), is the surface area of the photocatalyst. K_{surf} provides the net heterogeneous process efficiency, taking into account the area of the photocatalyst that can be utilized for decomposition processes.

K_{surf} values calculated from Eq. (9) are summarized in Table 2. The K_{surf} values for all particles are nearly the same, but the photoefficiency are different. These results suggest that the photocatalytic efficiency does not just depend on the amount of catalyst surface exposed to radiation, but also on the type and nature of this exposed surface in terms of the chemical composition and microstructure. In this regard, silicon and ruthenium behave differently with regard to the effect each has on TiO_2 in the composite materials. This treatment assumes that all of the photocatalyst material was uniformly illuminated.

We observe here that though the nanoparticles are effective towards the decomposition of the azo-dye, the efficiency of SiO_2 in enhancing the activity of TiO_2 appears to strongly depend on the presence of RuO_2 as well. In the absence of RuO_2, and for 10% (w/w) SiO_2 in the composite material, the percentage decomposition decreased by a factor of 3, from 28.2 to 9.8%. In the absence of RuO_2, TiO_2/SiO_2 is not an efficient composite nanocatalyst material. The reason for this could be that because SiO_2 is an amphoteric oxide, it could be charged at the experimental pH. The pH is related to the acid–base property of the metal oxide surface and can be explained on the basis of zero point charge. The adsorption of water molecules at surficial metal sites is followed by the dissociation of OH^- charge groups leading to coverage with chemically equivalent metal hydroxyl groups (M–OH) [31]. Due to the amphoteric behaviour of most metal hydroxides, the following equilibrium reactions could be invoked to explain the observed behaviour

$$\text{M–OH} + \text{H}^+ \rightarrow \text{M–OH}_2{}^+ \tag{10}$$

$$\text{M–OH} \rightarrow \text{M–O}^- + \text{H}^+ \tag{11}$$

It is possible that at pH of 8, the surface of SiO_2 is positively charged and the formation of OH radicals, the principal

Table 2
Kinetic parameters and photocatalytic efficiency (%) of TiO_2 nanoparticles towards MO degradation

	TiO_2 foam	TiO_2 (SiO_2, 10%)	RuO_2/TiO_2	RuO_2/TiO_2 (SiO_2, 5%)	RuO_2/TiO_2 (SiO_2, 10%)
Degradation after 1 h illumination (%)	47.1	24.6	50.1	75.5	106.4
k_{app}, rate constant (min^{-1})	0.370	0.376	0.415	0.429	0.530
k_{surf} ($cm^{-2}\,min^{-1}$) × 10^{-4}	3.06	2.91	2.70	2.90	3.01
Time for complete decolorization (min)	127.3	245.4	100	79.5	57.2
R^2	0.9220	0.9601	0.9601	0.9947	0.9974

oxidizing species, is not favoured and hence photoefficiency is not enhanced with respect to SiO_2 [32] due to its inability to generate e–h pairs on the surface. In terms of efficiency, the rate constants and percentage decomposition of MO decreased in the order TiO_2/RuO_2 (SiO_2 10%, w/w) > TiO_2/RuO_2 (SiO_2 5%, w/w) > TiO_2/RuO_2 (90:10%, w/w) > TiO_2/SiO_2 (90:10%, w/w).

It was observed that RuO_2 concentration less than 5% (w/w) in TiO_2 did not result in significant decolorization of MO. On the other hand, increasing the concentration of RuO_2 more than 10% (w/w) in TiO_2 did not result in any proportionate increase in photocatalytic activity either. Similarly, increasing the SiO_2 loading in the composite more than 10% (w/w) did not result in any photocatalytic benefit. This has also been observed with gold and silver modification of TiO_2 [16,33].

3.6. Photocatalytic activity of TiO_2 foam

Different loads of TiO_2 foam were evaluated for their catalytic activity towards MO decomposition and Fig. 5(a–c) show the photodecomposition kinetic data. The kinetic plots indicate photocatalytic rate dependence on the amount of catalyst used, with percentage decomposition (decrease in MO concentration) varying from 95.8% with 9 g of foam, 71.4% with 2 g of foam, 35.7% with 0.5 g of foam to 29% with 0.2 g of foam. After 100 min of irradiation, the 95.8% of decomposition achieved with 9 g of foam, compared to 29% obtained for 0.2 g of foam, represented only a 3.4-fold increase in decomposition compared to a 45-fold increase in catalyst load. The semi-logarithmic plot shown in Fig. 5(a) gave a straight line with R^2 values ranging from 0.9977 to 0.9988 while Fig. 5(c) shows a decrease in MO concentration with time in accord with first order kinetics.

Results show that the same loads of TiO_2 foams in different concentrations of MO produced different photocatalytic effects. The rate of decomposition was higher with 5 mg/l MO than with 10 mg/l dye, but lower with 1 mg/l dye (not shown). Therefore, the ability of the photocatalyst to decompose the dye should be determined by comparing the initial decomposition rates upon illumination as explained earlier. Concentrations of methyl orange more than 10 mg/l were also studied but no marked differences in the rate of degradation were observed. This has been reported in similar studies [34]—where it was observed that for dye concentrations of 5–10 mg/l, almost 100% complete degradation occurred within 60 and 120 min of irradiation. However as the concentration was increased, the time for complete degradation was observed to increase significantly; to 4 h using 25 mg/l concentration of MO. The explanation for this is that as the initial concentration of the dye increases, the path length of the photons entering the solution decreases leading to a slow-down or decrease in photocatalytic efficiency as the catalyst load increases [34]. The same effect has been observed by Neppolian et al. [35] in a study of the degradation of three commercial textile dyes (Reactive Yellow, Reactive Red and Reactive Blue) using TiO_2 photocatalysts.

3.7. Comparison with commercial TiO_2

The photocatalytic activity of commercial TiO_2 (Degussa P-25) has been studied extensively and compared with stud-

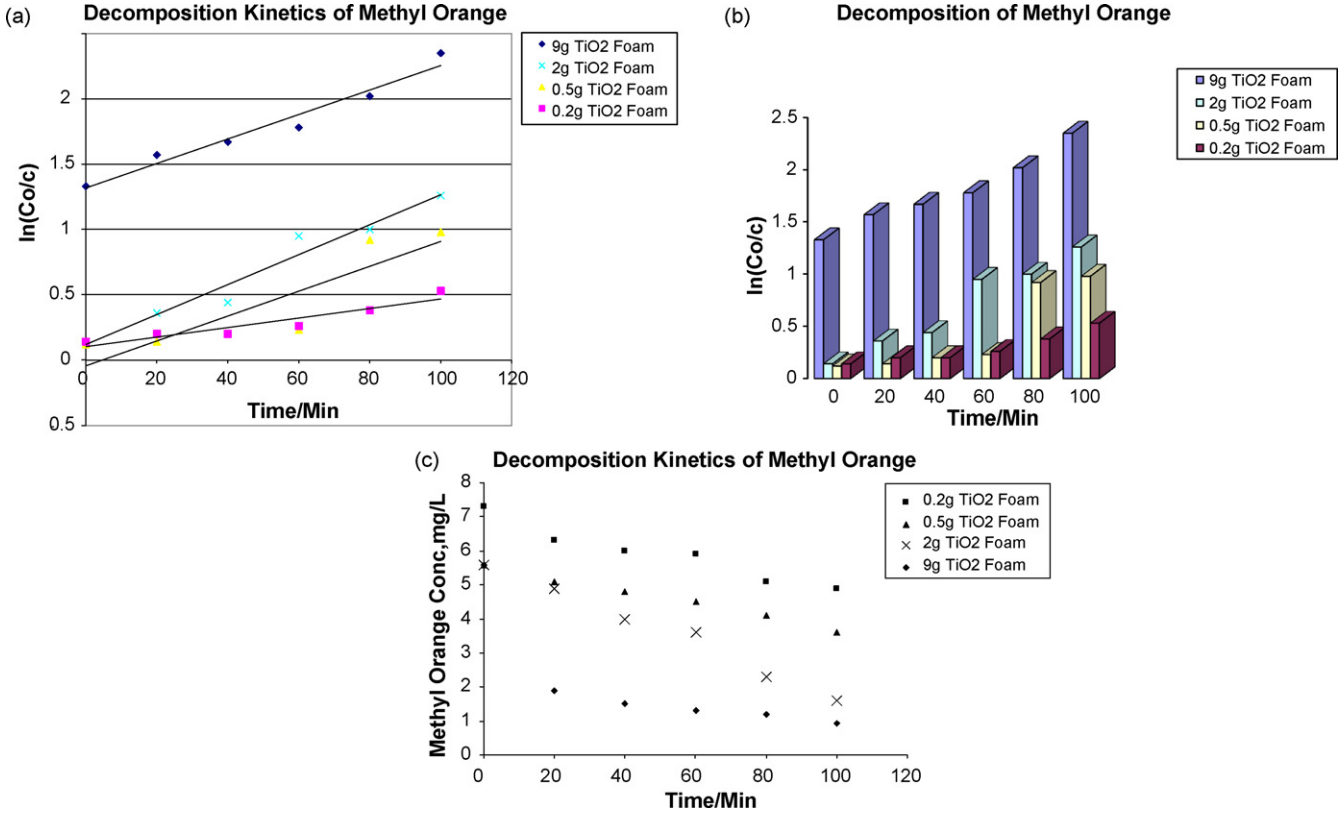

Fig. 5. (a–c) Decomposition kinetics of MO in titania foam.

ies carried out with silver modified TiO_2 [20], gold modified TiO_2 [28] and these studies came to essentially the same conclusions, broadly in agreement with the results of the present study. The modified materials were observed to be more efficient than the commercial TiO_2. For example, published work on methyl orange using pure TiO_2, gold and silver modified TiO_2 materials, indicate that for the modified materials, the time to completely decolorize methyl orange was twice as fast as for pure TiO_2. In addition, the percentage decolorization after 1 h of illumination was 34.5% for pure TiO_2 compared to 90% for gold modified TiO_2. The rate constant and time for complete decolorization were 0.0103 min^{-1} and 330 min for pure TiO_2 [28]. In this study, the percentage degradation after 1 h of illumination was 47.15% for TiO_2 foam, 75.5 and 106.4%, respectively, for TiO_2/RuO_2 (SiO_2 5%, w/w) and TiO_2/RuO_2 (SiO_2 10%, w/w) compared to 34.15% for commercial TiO_2.

The reasons given for the better performance of the modified materials compared to commercial TiO_2 was that in addition to the reduction in the band gap energy of titania due to the incorporation of silver or gold particles, the surface properties of the titania were also modified as a result, bringing about a simultaneous reduction in band gap energy and improved surface properties [36]. The results obtained in this study can thus be explained on the basis that RuO_2 and SiO_2 served the dual purpose of a simultaneous reduction in band gap energy and increase in the surface area of TiO_2. Some studies, based on AFM, SEM, and XRD analysis alone, have suggested that the improved activity of modified TiO_2 materials is due exclusively to improved surface properties of the modified TiO_2 [37]. These composite materials as well as the foam should be contaminant non-specific and hence can be applied to the treatment of low levels of pollutant organics in water and air including pesticides, rhodamine, metachlor, trichloroethylene, chlorophenol, xylene, benzene, toluene and nitrogen containing pollutants, etc.

3.8. TiO_2 surface morphology and catalytic activity

Rough, high surface area titania materials including foams and films, show a great ability to efficiently capture protons through a thick semiconducting network. This 'sponge' like architecture and porosity of the foam, for example, explain the enhanced photocatalytic efficiency observed with modified titania material. On the other hand, the TiO_2/RuO_2 (SiO_2 10%) presents a composite surface which has a dual function as photons capturing material and as SiO_2/RuO_2 promoted substrate.

The surface coverage and the diameter of the particles presented in Table 2 are crucial parameters to also take into account [38–48] and the results of this study indicate that in terms of photocatalytic activity, SiO_2 and RuO_2 appear to have a synergistic relationship as they appear to 'cooperate' to enhance the photocatalytic activity of TiO_2. With respect to the titania foam, the highly porous and rough structure makes it ideal for volatile organic compound (VOC) remediation in air and water although degradation rates appear to slowdown with time, due possibly to deterioration in catalytic activity. The mechanism of decomposition of methyl orange using the titania foam is far more complex and this is under investigation, including details of the porosity and network architecture.

4. Conclusions

X-ray diffractive measurements and SEM characterization of the titania foam show very rough and porous surfaces properties. These enhance the photocatalytic activity of TiO_2 foam towards azo-dye degradation. The photocatalytic activity improved significantly with an increase in the amount of foam used as well as the time of radiation. The photocatalytic behaviour and properties of a series of TiO_2/RuO_2 particles obtained by hydrogen reduction reactions indicate that a combination of TiO_2/RuO_2 and SiO_2 particles is a more efficient photocatalyst for the decomposition of methyl orange than TiO_2 alone. Silicon dioxide and ruthenium dioxide appear to work cooperatively in enhancing the photocatalytic activity of titanium dioxide.

Acknowledgements

The financial support from the Greek–British partnership programme is gratefully acknowledged. Thanks are due the technicians in Chemistry Department for the Raman investigations and assistance with XRD, AFM and SEM measurements. Thanks are due to Degussa, Macclesfield, England, United Kingdom for the P-25 sample.

References

[1] V.E. Henrich, P.A. Cox, The Surface Science of Metal Oxides, Cambridge University Press, Cambridge, 1994.
[2] C. Noguera, Physics and Chemistry of Oxide Surfaces, Cambridge University Press, Cambridge, 1996.
[3] U. Diebold, J. Appl. Phys. A 76 (2002) 1–7.
[4] C.T. Campbell, Surf. Sci. Rep. 27 (1997) 1.
[5] M.A. Fox, M.T. Dulay, Chem. Rev. 93 (1993) 341.
[61] M.R. Hoffman, S.T. Martin, W. Choi, D.W. Bahnemann, Chem. Rev. 95 (1995) 69.
[7] A.L. Linsbigler, G. Lu, J.T. Yates Jr., Chem. Rev. 95 (1995) 735.
[8] A. Hagfeldt, M. Gratzel, Chem. Rev. 95 (1995) 49.
[9] N. Chandrasekharan, P.V. Kamat, J. Phys. Chem. B 104 (2000) 10851.
[10] V. Subramanian, E. Wolf, P.V. Kamat, J. Phys. Chem. B 105 (2001) 11439.
[11] M. Date, Y. Ichihashi, T. Yamashita, A. Chiorino, F. Boccuzzi, M.M. Haruta, Catal. Today 72 (2002) 89.
[12] M. Valden, X. Lai, D.W. Goodman, Science 281 (1998) 1647.
[13] M. Muruganandham, M. Swaminatham, Dyes Pigm. 62 (2004) 269.
[14] C. Baiocchi, C.M. Brussimo, E. Praumauro, A.B. Prevot, L. Palmisano, G. Marci, Int. J. Mass Spectrom. 214 (2002) 247.
[15] H. Zoolinger, Colour Chemistry: Synthesis, Properties and Applications of Organic Dyes and Pigments, VCH Publishers, New York, 1987.
[16] C. Baiocchi, M.C. Brussino, E. Pramauro, A.B. Prevot, L. Palmisano, G. Marci, J. Mass Spectrom. 214 (2002) 247.
[17] I.M. Arabatzis, T. Stergiopolous, M.C. Bernard, D. Labou, S.G. Neophytides, P. Falaras, Appl. Catal. B: Environ. 42 (2003) 187–210.
[18] I.M. Arabatzis, P. Falaras, Nanoletters 3 (2) (2003) 249–251.
[19] J. Zhao, X.D. Yang, Building Environ. 38 (2003) 645–654.
[20] I.M. Arabatzis, T. Stergiopoulos, D. Andreeva, S. Kitova, S.G. Neophytides, P. Falaras, J. Catal. 220 (2003) 127–135.
[21] H.K. Yoon, S.J. Noh, C.H. Kwon, M. Muhammed, Mater. Chem. Phys. 95 (1) (2006) 79–83.
[22] C. Anderson, A.J. Bard, J. Phys. Chem. 99 (1995) 9882.

[23] H. Zhang, J.F. Banfield, J. Phys. Chem. B 104 (2000) 3481.
[24] R.W. Matthews, J. Phys. Chem. 91 (1987) 3328–3333.
[25] R.W. Matthews, Solar Energy 38 (1987) 405–413.
[26] W.A. Jacoby, Ph.D. Dissertation, University of Colorado, USA, 1993.
[27] N. Daneshar, D. Salari, A.R. Khatae, J. Photochem. Photobiol. A: Chem. 157 (2003) 111.
[28] V.A. Sakkas, I.M. Arabatzis, I.K. Konstantinou, A.D. Dimou, T.A. Albanis, P. Falaras, Appl. Catal. B: Environ. 49 (2004) 195–205.
[29] G. Katsaros, T. Stergiopoulos, I.M. Arabatzis, K.G. Ppadokostaki, P. Falaras, J. Photochem. Photobiol. A149 (2002) 191.
[30] P. Falaras, A.P. Xagas, J. Mater. Sci. 37 (2002) 3855.
[31] W. Stumin, J.J. Morgan, Aquatic Chemistry, Wiley, New York, 1981.
[32] A. Akyoi, H.C. Yatmaz, M. Bayramoglu, Appl. Catal. B: Environ. 54 (2004) 19.
[33] J.M. Herman, H. Tahiri, Y. Ait-Ichou, G. Lassaletta, A.R. Gonzalez-Elipe, A. Fernandez, Appl. Catal. B: Environ. 13 (1997) 219.
[34] R.J. Davies, J.L. Gainer, G.O. Neal, I.W. Wu, Water Environ. Res. 66 (1994) 50.
[35] B. Neppolian, H.C. Choi, S. Sakthivel, B. Arabindoo, V. Murugesan, J. Hazard. Mater. B 89 (2002) 303.
[36] H. AL-Ekabi, N. Serpone, J. Phys. Chem. 92 (1988) 5726.
[37] W. Ma, Z. Lu, M. Zhang, Appl. Phys. A 66 (1998) 621.
[38] A. Gajovic, M. Ivanda, A. Drasner, Thin Solid Films 198 (1991) 199.
[39] N. Serpone, D. Lawless, R. Khairutdinov, E.E. Pelizzetti, J. Phys. Chem. 99 (1995) 16655.
[40] S.J. Masten, S.H.R. Davies, Environ. Sci. Technol. 28 (1994) 180–185.
[41] H.Y. Hsieh, J. Chemosphere 36 (1998) 2763–2773.
[42] T.N. Obee, S.O. Hay, Environ. Sci. Technol. 31 (1997) 2034–2038.
[43] A.O. Ibhadon, G.M. Greenway, Y. Yue, Catal. Commun. 9 (2008) 153–157.
[44] X.Z. Li, F.B. Li, Environ. Sci. Technol. 35 (2001) 2381.
[45] F. Boccuzzi, A. Chiorino, M. Manzoli, D. Andreeva, T. Tabakova, L. Iiieva, V. Idakiev, Catal. Today 72 (2002) 169.
[46] D. Andreeva, T. Tabakova, L. Iiieva, V. Idakiev, P. Falaras, A. Bourlinos, A. Travlos, Catal. Today 72 (2002) 51.
[47] W.H. Glaze, Environ. Sci. Technol. 21 (1987) 224–230.
[48] O. Legrini, E. Oliveros, A. Braun, Chem. Rev. 93 (1993) 671–698.